Monthly Notices
of the
ROYAL ASTRONOMICAL SOCIETY

MNRAS **429,** 2924–2933 (2013) doi:10.1093/mnras/sts501

How do minor mergers promote inside-out growth of ellipticals, transforming the size, density profile and dark matter fraction?

Michael Hilz,[1] Thorsten Naab[1]⋆ and J. P. Ostriker[2]

[1]*Max-Planck-Institut für Astrophysik, Karl-Schwarzschild-Str. 1, D-85741 Garching, Germany*
[2]*Department of Astrophysical Sciences, Princeton University, Princeton, NJ 08544, USA*

Accepted 2012 November 27. Received 2012 November 26; in original form 2012 June 20

ABSTRACT

There is observational evidence for inside-out growth of giant elliptical galaxies since $z \gtrsim$ 2–3, which is – in contrast to disc galaxies – not driven by in situ star formation. Many of the $\sim 10^{11}$ M$_\odot$ systems at high redshift have small sizes $\sim$1 kpc and surface brightness profiles with low-Sérsic indices n. The most likely descendants at $z = 0$ have, on average, grown by a factor of 2 in mass and a factor of 4 in size, indicating $r \propto M^\alpha$ with $\alpha \gtrsim 2$. They also have surface brightness profiles with $n \gtrsim 5$. This evolution can be qualitatively explained on the basis of two assumptions: compact ellipticals predominantly grow by collisionless minor (mass-ratio 1:10) or intermediate (mass-ratio 1:5) 'dry' mergers, and they are embedded in massive dark matter haloes which support the stripping of merging satellite stars at large radii. We draw these conclusions from idealized collisionless mergers spheroidal galaxies – with and without dark matter – with mass ratios of 1:1, 1:5 and 1:10. The sizes evolve as $r \propto M^\alpha$ with $\alpha < 2$ for mass-ratios of 1:1 (and 1:5 without dark matter haloes) and, while doubling the stellar mass, the Sérsic index increases from $n \sim 4$ to $n \sim 5$. For minor mergers of galaxies embedded in dark matter haloes, the sizes grow significantly faster and the profile shapes change more rapidly. Surprisingly, already mergers with moderate mass-ratios of 1:5, well motivated by recent cosmological simulations, give $\alpha \sim 2.3$ and after only two merger generations ($\sim$40 per cent added stellar mass) the Sérsic index has increased to $n > 8$ ($n \sim 5.5$ without dark matter), reaching a final value of $n = 9.5$ after doubling the stellar mass. This is accompanied by a significant increase of the dark matter fraction (from $\sim$40 to $\gtrsim$70 per cent) within the stellar half-mass radius, driven by the strong size increase probing larger, dark matter-dominated regions. For equal-mass mergers the effect is much weaker. We conclude that only a few intermediate mass-ratio mergers ($\sim$3–5 with initial mass-ratios of 1:5) of galaxies embedded in massive dark matter haloes can result in the observed concurrent inside-out growth and the rapid evolution in profile shapes. This process might explain the existence of present-day giant ellipticals with sizes, $r > 4$ kpc, high Sérsic indices, $n > 5$, and a significant amount of dark matter within the half-light radius. Apart from negative stellar metallicity gradients such a 'minor' merger scenario also predicts significantly lower dark matter fractions for $z \sim$ 2 compact quiescent galaxies and their rare present-day analogues.

Key words: galaxies: ellipticals and lenticular, cD – galaxies: evolution – galaxies: fundamental parameters – galaxies: haloes – galaxies: photometry – galaxies: structure.

1 INTRODUCTION

Merging is a natural process in hierarchical cosmological models and plays a significant role for the assembly of massive galaxies (e.g. Kauffmann 1996). The most massive objects are elliptical galaxies, which are considered to start forming their stars at a redshift of $z \sim 6$ in a dissipative environment and can rapidly become very massive ($\sim 10^{11}$ M$_\odot$) by $z = 2$ (Kereš et al. 2005, 2009; De Lucia et al. 2006; Khochfar & Silk 2006; Kriek et al. 2006; Naab et al. 2007; Dekel, Sari & Ceverino 2009; Joung, Cen & Bryan 2009; Naab, Johansson & Ostriker 2009; Feldmann et al. 2010; Oser et al. 2010; Domínguez Sánchez et al. 2011; Feldmann, Carollo & Mayer 2011; Oser et al. 2012). Their subsequent evolution is not fully understood yet, as these ellipticals are observed to be already quiescent at $z \sim 2$, on average four to five times smaller, and a factor of 2 less massive

⋆ E-mail: naab@mpa-garching.mpg.de

than their low-redshift descendants (Daddi et al. 2005; Trujillo et al. 2006; Longhetti et al. 2007; Toft et al. 2007; Trujillo et al. 2007; Zirm et al. 2007; Buitrago et al. 2008; Cimatti et al. 2008; Franx et al. 2008; van Dokkum et al. 2008, 2010; Bezanson et al. 2009; Damjanov et al. 2009; Kriek et al. 2009; Saracco, Longhetti & Andreon 2009; Saglia et al. 2010; Onodera et al. 2012; Whitaker et al. 2012). This rapid size evolution eventually proceeds in an inside-out fashion in the absence of significant star formation and is accompanied by an evolution in the light (and eventually mass) distribution (Hopkins et al. 2009a; van Dokkum et al. 2010; Auger et al. 2011; Tiret et al. 2011; Saracco, Gargiulo & Longhetti 2012; Szomoru, Franx & van Dokkum 2012). This growth process is distinctively different from the star formation-driven inside-out growth of disc galaxies (Matteucci & Francois 1989; Prantzos & Aubert 1995; Mo, Mao & White 1998; Naab & Ostriker 2006; Governato et al. 2007; Wang et al. 2011; Kauffmann et al. 2012). In addition, there is growing observational evidence that high-redshift ellipticals are more flattened with exponential-like surface brightness distributions ($n \lesssim 4$) whereas their potential present-day massive descendants are rounder and have more concentrated profiles shapes with $n \gtrsim 5$ (Toft et al. 2005, 2007; Trujillo et al. 2006; van Dokkum et al. 2008, 2010; van der Wel et al. 2008, 2009a, 2011; Kormendy et al. 2009; Carrasco, Conselice & Trujillo 2010; Buitrago et al. 2013; Weinzirl et al. 2011; Kormendy & Bender 2012; Szomoru et al. 2012).

Direct observations of massive compact and quiescent high-redshift systems also provide new constraints on the formation histories of giant elliptical galaxies. At face value, the dramatic difference in properties of massive quiescent galaxies at high and low redshift rules out a simple 'monolithic' formation followed by simple passive evolution (Kriek et al. 2008; van Dokkum et al. 2008). The observations also rule out the formation of ellipticals in a single 'disc merger' event, a scenario for massive ellipticals which might also suffer from other problems (Ostriker 1980; Naab & Burkert 2003; Burkert et al. 2008; Naab & Ostriker 2009). Even if the progenitor discs were gas rich leading to a compact remnant (Ricciardelli et al. 2010; Wuyts et al. 2010; Bournaud et al. 2011), those would have to evolve further by a separate process (see e.g. Hopkins et al. 2009a).

In addition to the well-studied stellar components, there is evidence for the existence for dark matter within the half-light radii of ellipticals (Gerhard et al. 2001; Thomas et al. 2009, 2011; Cappellari et al. 2012a). Gravitational lensing measurements of massive galaxies in the local Universe predict, on average, ∼30 per cent of the matter within the half-light radius of present-day massive elliptical galaxies being dark matter (Auger et al. 2010; Barnabè et al. 2011). At high redshift, however, the situation is more uncertain (Toft et al. 2012) as dark matter cannot be measured directly. The naive expectation is that dark matter is much less important due to the dissipative nature of the early evolution. Still, assuming its existence and collisionless nature, dark matter will eventually affect the distribution of stars during the further assembly of the galaxies (see e.g. Lackner & Ostriker 2010; Hilz et al. 2012).

The underlying idealized assumption for the study presented here is that present-day massive elliptical galaxies ($>10^{11}\,M_{\odot}$) since $z \sim 2$ have grown predominantly by accreting stars that have formed in other galaxies and this process can be approximated by simulations of mergers of collisionless 'dry' stellar systems. This assumption is not too far fetched as there is clear observational evidence for the predominance of old ($z \gtrsim 2$) stellar populations in these galaxies, leaving little room for gas accretion and subsequent star formation (e.g. Searle, Sargent & Bagnuolo 1973; Brinchmann & Ellis 2000; Treu et al. 2005; López-Sanjuan et al. 2010; Thomas et al. 2010; van Dokkum et al. 2010; Young et al. 2011; Crocker et al. 2012). Directly observed mergers, inferred merger rates, as well as stellar fine structure at large galactocentric radii are indicative of stellar merger and accretion events (Malin & Carter 1983; Schweizer & Seitzer 1992; Tran et al. 2005; van Dokkum 2005; Bell et al. 2006a,b; Faber et al. 2007; McIntosh et al. 2008; Whitaker & van Dokkum 2008; Robaina et al. 2010; Duc et al. 2011; Lotz et al. 2011; Trujillo, Ferreras & de La Rosa 2011; Weinzirl et al. 2011; Tal et al. 2012). On the theoretical side, phenomenological as well as direct numerical studies predict that the late assembly of massive galaxies is dominated by the late accretion of stars that formed early (Kauffmann 1996; De Lucia et al. 2006; Ciotti, Lanzoni & Volonteri 2007; Naab et al. 2007, 2009; Guo & White 2008, 2012, Lackner & Ostriker 2010, Oser et al. 2010, 2012, Feldmann et al. 2011; Guo et al. 2011; Yang et al. 2012; Gabor & Davé 2012; Lackner et al. 2012; Moster, Naab & White 2012). In a previous study, Hilz et al. (2012) used idealized merger simulations of spheroidal galaxies to re-investigate the effect of the galaxy merger mass-ratio – limited to the extreme cases of 1:1 and 1:10 – on the merger-driven evolution of compact high-redshift spheroids. The main finding of this study was that both minor and major mergers lead to size growth and an increase of the dark matter fraction, however, by different physical processes and at significantly different strengths. Violent relaxation in major mergers mixes dark matter into the central regions and escaping particles limit the expected size growth even below the expected values. In 1:10 mergers on the other hand, satellite particles are stripped at large radii where the initial host galaxies are dominated by dark matter. As a result the stellar effective radii and the dark matter fractions of the galaxies grow rapidly.

Here we extend the Hilz et al. (2012) study to focus on the inside-out growth including a moderate mass-ratio of 1:5. This step is important for a number of reasons: The average stellar mass growth since $z \sim 2$ is a factor of 2. Mergers with mass-ratios of 1:10 typically take a long time to complete and it is not clear whether 10 of these mergers can even be completed in a Hubble time. Additionally, recent observationally estimated merger rates indicate more minor mergers for massive galaxies and at higher redshift but the rates are still low and it is not clear – also theoretically – whether there are enough minor mergers to explain the size growth (Nipoti et al. 2009a; Nipoti, Treu & Bolton 2009b; Weinzirl et al. 2011; Williams, Quadri & Franx 2011; Cimatti, Nipoti & Cassata 2012; Edwards & Patton 2012; Man et al. 2012; Mármol-Queraltó et al. 2012; Newman et al. 2012; Nipoti et al. 2012). Higher mass-ratio mergers result in a more rapid mass growth and fewer of them would be needed provided the size grows rapid enough. Another reason to focus on mass-ratios of 1:5 was recently provided by direct cosmological simulations. Three independent numerical studies have found that the average mass-weighted mass ratio of galaxy mergers building massive ellipticals is 1:4–1:5, making this regime particularly interesting (Gabor & Davé 2012; Lackner et al. 2012; Oser et al. 2012).

In Section 2, we give a short review of the initial galaxy models and the simulation parameters. In the subsequent Sections 3, 4, 5 and 6, we investigate the evolution of sizes, surface densities, profiles shapes and dark matter fractions, respectively. We discuss the results and conclude in Section 7.

2 SIMULATIONS

Continuing the long line of research in this direction (White 1978, 1979; Miller & Smith 1980; Farouki, Shapiro & Duncan 1983; Villumsen 1983; Nipoti, Londrillo & Ciotti 2003; Boylan-Kolchin,

Ma & Quataert 2005; Ciotti et al. 2007; Nipoti et al. 2009b), we present a set of simulations of dissipationless mergers of spheroidal galaxies with and without dark matter haloes and with mass ratios of 1:1, 1:5 and 10:1. Details about the initial models and the simulation parameters for 1:1 and 1:10 mergers are presented in Hilz et al. (2012). The simulations were performed with the *N*-body/SPH code VINE (Nelson, Wetzstein & Naab 2009; Wetzstein et al. 2009). For this study, we have also performed comparison run with GADGET (Springel 2005) with identical results. Here, we only give a brief summary of the simulation setup. The initial galaxy models are isotropic, spherically symmetric one- and two-component systems following Hernquist density profiles (Hernquist 1990) either for a model representing only the stellar component of the galaxy (one-component, bulge only) or a bulge embedded in a massive dark matter halo (two-component, bulge+halo). The host bulges have a stellar mass of $M_{\star,\,\mathrm{host}} = 1$ and a scale radius of $a_{\star,\,\mathrm{host}} = 1.0$ [corresponding to a projected half-mass radius of $R_\mathrm{e} \sim 1.8 a_{\star,\,\mathrm{host}}$ (Hernquist 1990) realized with 100 000 particles]. For the two-component cases, we assume an additional dark matter halo with a total dark to stellar mass ratio of $M_\mathrm{dm}/M_\star = 10$ and a ratio of the scale radii of $a_\mathrm{dm}/a_\star = 11$. The halo is realized with 1000 000 particles resulting in equal-mass particles for both components. The gravitational softening length is set to $\epsilon = 0.02$ for all particles. The stability of the initial *N*-body models was demonstrated in Hilz et al. (2012). The merging satellite galaxies are five (mass-ratio 1:5) or ten times (mass-ratio 1:10) less massive than the host and have a correspondingly lower particle number. For our fiducial set of simulations, we assume the same scale radius, $a_{\star,\,\mathrm{sat}} = 1.0$, for all bulges, resulting in satellites being more diffuse than the host. For a second set of simulations, we choose more compact satellites with scale radii of $a_{\star,\,\mathrm{sat}} = 0.8$ for the 1:5 mergers and $a_{\star,\,\mathrm{sat}} = 0.5$ for the 1:10 mergers following a $z \sim 2$ mass–size relation (Williams et al. 2010).

The open and filled circles in Fig. 1 indicate the location of the initial galaxy models in the mass–size plane compared to several published present-day and high-redshift mass–size relations. The initial massive host galaxies resemble typical massive and compact 'red nuggets' at $z = 2$ which are smaller than typical present-day galaxies at $10^{11}\,\mathrm{M}_\odot$ (red line from Williams et al. 2010). However, for redshift two galaxies below $\sim 4.0 \times 10^{10}\,\mathrm{M}_\odot$ (which would be the minor merger partners), there is no consistent size information available. Therefore, we assume two scenarios: a fixed size of $\sim$1 kpc for the satellites, similar to local galaxies (see e.g. Misgeld & Hilker 2011), indicated by the filled red and green circles. Here, the merging lower mass galaxies are diffuse spheroids with low phase-space densities comparable to low-mass disc-like galaxies. Alternatively, we use smaller sizes consistent with a simple continuation of the $z = 2$ mass–size relation to lower masses (open circles), resulting in compact spheroids.

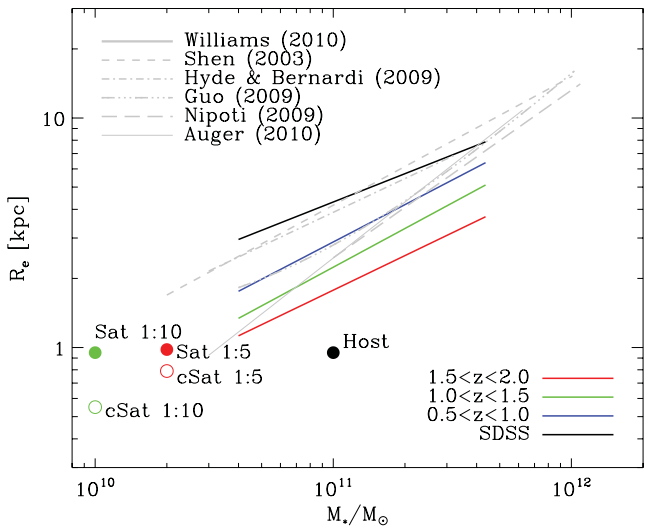

Figure 1. Stellar mass versus effective radius for the initial galaxy models. For our fiducial set of simulations (diffuse satellites), all galaxies have an effective radius of 1 kpc (filled circles). For the second set of simulations with compact satellites (open circles), the sizes follow the $z = 2$ relation (red line) by Williams et al. (2010). The initial conditions are well separated from local mass–size relations of ellipticals (Shen et al. 2003; Guo et al. 2009; Hyde & Bernardi 2009; Nipoti et al. 2009a; Auger et al. 2010).

The first generation of equal-mass mergers are parabolic mergers of one- and two-component models of the initial host galaxies. The second generation is a re-merger of the duplicated, randomly oriented, first generation merger remnant, which was allowed to dynamically relax at the centre. The randomly oriented galaxies approach each other on parabolic orbits with a pericentre distance of half the spherical half-mass radius of the progenitor remnants, i.e. the pericentre distances increase with each merger generation. The sequences of intermediate and minor mergers with initial mass-ratios of 1:5 (1:10) are also simulated with one- and two-component models. In the following, we use the traditional convention to call all mergers with mass-ratios smaller than 1:4 minor mergers. Initially, the mass-ratio is 1:5 (1:10) and the galaxies are set on parabolic orbits. The randomly oriented merger remnants of the first generations are then set on parabolic orbits with the initial satellite galaxy models and a mass-ratio of now 1:6 (1:11), and so on. We perform six generations of 1:10 mergers and five generations of 1:5 mergers using satellites with fixed scale radii (Sat 1:5/1:10, see Fig. 1). For comparison, we also performed minor mergers of two-component models with compact satellites (cSat 1:5/1:10, see Fig. 1). Again all parabolic orbits have pericentre distances of half the spherical half-mass radius of the bulge of the massive progenitor galaxy.

The 1:10 bulge-only simulations have no dark matter halo and the in-falling satellites suffer less from dynamical friction. Therefore, the final coalescence takes by far the longest time. However, taking about $\sim$9 Gyr for 10 merger generations even this process could be completed by the present day assuming a $z = 2$ progenitor. All other merger series are completed in less than $\sim$7 Gyr.

3 EVOLUTION OF THE SIZES

After the completion of every merger, we allow the central region of the remnant to relax, before we compute the projected circular half-mass radii, r_e, along the three principal axes and the bound stellar (bulge) mass, $M_\star$.

In Fig. 2, we show the evolution of the half-mass radius as a function of the bound stellar mass for 1:1 (blue), 1:5 (red) and 1:10 (green) merger hierarchies. The black line indicates the observed evolution, $r_e \propto M^{2.04}$, in the mass–size plane from $z \sim 2$ to the present day (van Dokkum et al. 2010). The models here are idealized in the sense that they do not contain any dissipative component. If present, like in the 'real' Universe, this component would reduce the size growth per added mass (Dekel & Cox 2006). Therefore, we consider a model a failure if it occupies the shaded area in Fig. 1. Promising models have to lie above this line so that small amounts of gas – and therefore somewhat smaller sizes – can be tolerated.

Equal-mass mergers show an almost linear increase of size with mass, (see also Boylan-Kolchin et al. 2005; Ciotti et al. 2007;

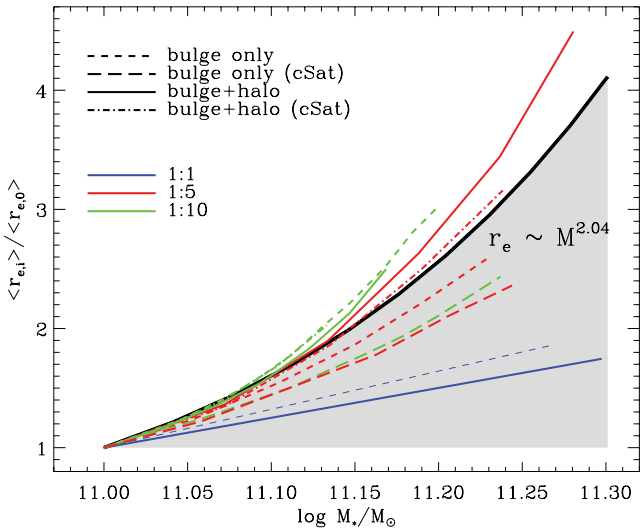

Figure 2. The projected spherical half-mass radius of the stellar component (the mean value along the three principal axes) as a function of bound stellar mass for 1:1 (blue), 1:5 (red) and 1:10 (green) mergers. The observed size growth is indicated by the solid black line [see van Dokkum et al. (2010) for the observational uncertainties]. The size evolution of models in the grey shaded area is too weak to be consistent with observations. All mergers of bulges embedded in massive dark matter haloes and high mass-ratios (1:5, 1:10, red and green solid/dash–dotted lines) show a rapid size evolution. The size evolution of the bulge-only models (short and long dashed lines) is not efficient enough, except the 1:10 scenario with a diffuse satellite (green dashed line). The accretion of compact satellites results in less size growth compared to the diffuse satellites. The major merger lines (blue) show size growth that is far too slow.

Bezanson et al. 2009; Nipoti et al. 2009b; Hilz et al. 2012), independent of whether the stellar system is embedded in a dark matter halo or not (blue solid and dashed lines). As discussed by Boylan-Kolchin et al. (2005), in mergers with dark matter haloes the in-falling galaxy suffers more from dynamical friction in the massive dark matter halo of the companion galaxy, resulting in more energy transfer from the bulge to the halo, leading to a more tightly bound bulge with a smaller size (blue solid line, Fig. 2) compared to the model without dark matter (blue dashed line, Fig. 2). If we combine the results of both major merger scenarios, this yields a mass–size relation of $r_e \propto M^{0.91}$ which is comparable to the results of Boylan-Kolchin et al. (2005), who found a slightly smaller exponent ($\sim$0.7) for orbits with high angular momentum and an exponent $\sim$1 for pure radial orbits. Nevertheless, as the size grows at most linearly with mass, dissipationless major mergers cannot be the main driver for the size evolution of early-type galaxies.

As expected from simple virial estimates (Cole et al. 2000; Ciotti et al. 2007; Bezanson et al. 2009; Naab et al. 2009), the size evolution is stronger for bulge-only models with lower mass-ratios of 1:5 and 1:10 (red and green lines in Fig. 2). However, except for the 1:10 mergers with a diffuse satellite (green short dashed line), all minor mergers with bulge-only satellites are not efficient enough to escape the 'forbidden' area. This behaviour is improved for minor mergers of two-component models, where bulges are embedded in a massive dark matter haloes. For mass-ratios 1:5 and 1:10 the size evolution is in excess of the observed evolution. In the case of 1:5 minor mergers with a less compact satellite (red solid line), we obtain a mass–size growth relation of $r_e \propto M^{2.4}$ with a similar or even larger exponent for both two-component 1:10 scenarios. Therefore, we consider all minor merger models (1:5 and 1:10) with dark matter haloes and the diffuse 1:10 mergers to be consistent with observations even in more realistic models, where dissipational effects would reduce the size growth (Cox et al. 2006; Robertson et al. 2006; Hopkins, Cox & Hernquist 2008; Covington et al. 2011). The size growth via major mergers is too slow to fit observational data.

4 EVOLUTION OF THE SURFACE DENSITIES

We now take a closer look at the evolution of the surface densities of the merger remnants. In Fig. 3, we plot the stellar surface mass densities and cumulative stellar mass profiles after every 1:1 and 1:5 merger and every second 1:10 merger for bulge-only models (top panels) and bulge+halo models (bottom panels). For equal-mass mergers, there is mass growth at all radii, i.e. the lines are shifted more or less parallel to higher densities independent of the presence of a halo (see e.g. Miller & Smith 1980; Farouki et al. 1983; Villumsen 1983 for discussions on the weak but existing break of homology). This evolution scenario would be in disagreement to observations of van Dokkum et al. (2010), which show, that early-type galaxies grow inside-out, i.e. the central densities stay constant and most of the mass assembles at larger radii, building up an extended envelope of stars.

The second column in Fig. 3 depicts the surface densities and mass assembly of minor mergers with an initial mass ratio of 1:5. For the bulge-only models (top) with a diffuse satellite (Sat 1:5, Fig. 2), the surface density stays nearly constant up to $r \sim 1 - 2$ kpc and increases mainly in the outer parts. This effect was already reported by Villumsen (1983) as a possible explanation for abundance gradients in elliptical galaxies. The same scenario leads to an even stronger inside-out growth if the galaxies are surrounded by a dark matter halo (bottom panel, second column). Here the bulge particles get stripped at larger radii and the central surface density ($r < 4$ kpc) stays unaffected; it only increases at radii $r > 2$–3 kpc. The size growth shown in Fig. 2 is due to this build-up of a massive stellar envelope. The mass is added to large radii where, prior to the merger, the dark matter component was large. Due to our accounting procedure, the dark matter fraction within r_e increases, even though the dark matter added in such mergers to the inner parts is negligible. The dotted lines in these panels show the four remnants, where the satellites are more compact (cSat 1:5, Fig. 2) and lie an extension of the $z \sim 2$ mass–size relation. Obviously, the results are very similar.

The six generations of minor mergers with an initial mass-ratio of 1:10 are shown in the right-hand column of Fig. 3. In the case of bulge-only models (top panels), the surface density increases predominantly at larger radii, similar to the previous scenario, but now the satellite stars are even less bound compared to the 1:5 case and therefore are stripped at larger radii, even without a dark matter halo. If present, this effect is enhanced (lower panels of right-hand column), as the satellites first orbit through the massive dark matter halo – and lose stars – before they reach the centre of the host. The surface densities are unaffected inside $r = 5$ kpc. In summary, 1:5 and 1:10 mergers lead to a significant change in the mass distribution of the galaxies with most of the stellar satellite material assembling at large radii. This picture hardly changes for compact satellites (cSat, dotted lines), although the scalelengths of the satellite stars are significantly smaller, they are more bound and resists the drag force of the host potential for a longer time. Consequently, somewhat more material gets closer to the central regions. In summary, a minor merger-driven evolution scenario – in particular for 1:5 bulge+halo mergers – is in good agreement with the picture we get from observations. Although we are definitely affected by poor

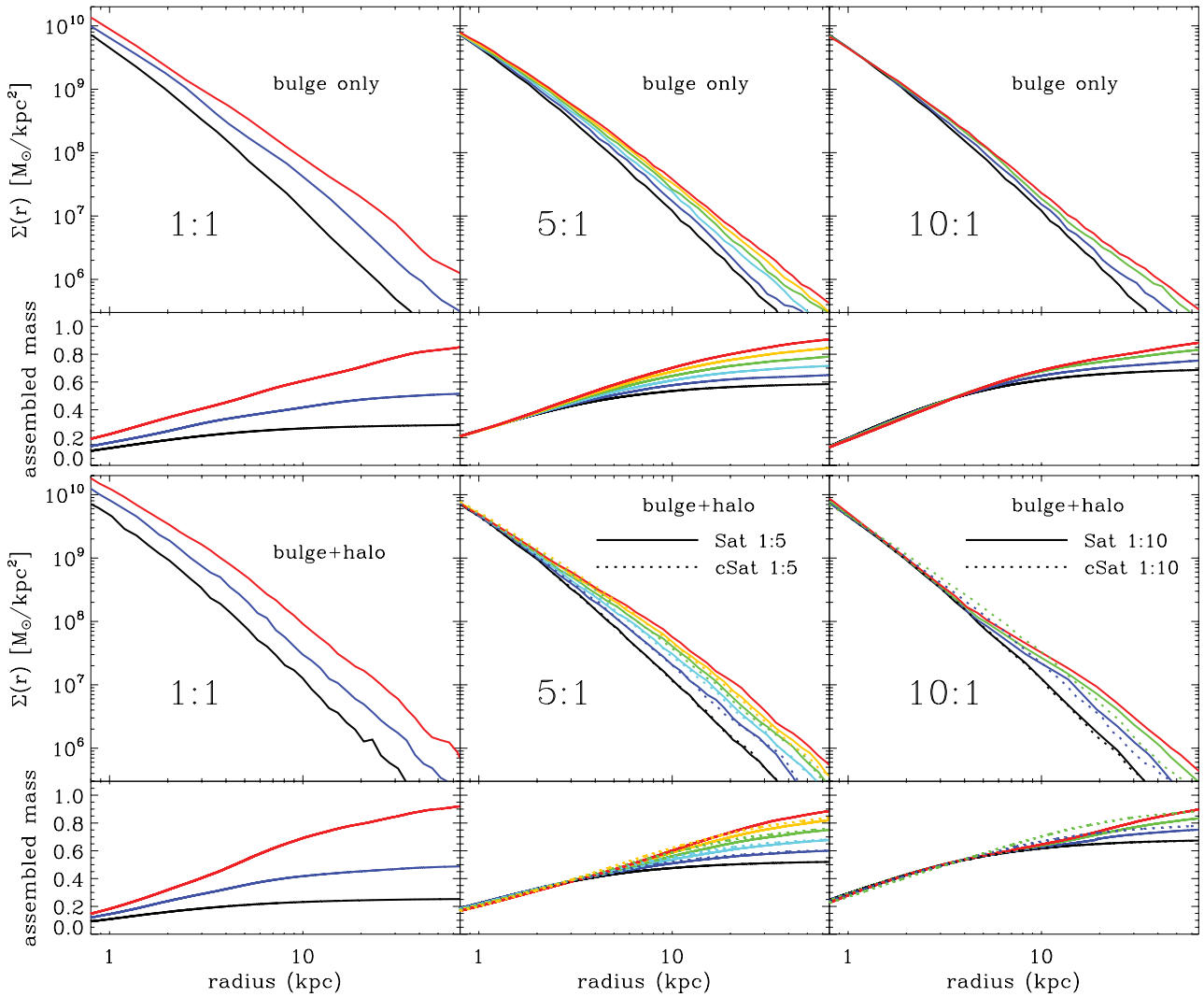

Figure 3. Top panels: stellar surface mass density profiles and cumulative stellar mass distributions for the fiducial 1:1 (left), 1:5 (middle) and 1:10 (right) bulge-only merger models after each merger event (coloured lines from bottom to top, for 1:1 and 1:5 mergers we show every generation, for 1:10 mergers every second). For all mass-ratios the surface densities increase at all radii with merger generation with a trend of a stronger increase in the outer regions for lower mass-ratios. Bottom panels: same for mergers of systems with dark matter haloes. Equal-mass mergers show a similar behaviour than bulge-only models. For 1:5 and 1:10 bulge+halo models (mergers with compact satellites are indicated by the dotted lines), the inside-out growth trend is stronger than for bulge-only models. Regions inside 4 kpc are almost unaffected and the satellite stellar mass assembles predominantly at large radii similar to observations van Dokkum et al. (2010).

numerical resolution at the very centres of the galaxies, we note the differential effect that for minor mergers the central surface densities decline the most even as the outer surface densities (and Sérsic indices) increase in agreement with expectations from recent observations (Szomoru, Franx & van Dokkum 2012; Trujillo, Carrasco & Ferré-Mateu 2012).

5 EVOLUTION OF PROFILE SHAPES

The curvature of the light profiles of elliptical galaxies is an important parameter as it correlates with other observed properties of elliptical galaxies, such as the effective radius r_e, the total luminosity and the stellar mass (Caon, Capaccioli & D'Onofrio 1993; Nipoti et al. 2003; Naab & Trujillo 2006; Kormendy et al. 2009. We therefore use a Sérsic $r^{1/n}$ (Sersic 1968) function to fit synthetic surface brightness profiles of our simulations,

$$I(r) = I_e \cdot 10^{-b_n((r/r_e)^{1/n}-1)}, \quad (1)$$

where the three free parameters are the effective surface brightness I_e, the effective radius r_e and the so-called Sérsic index n. Here, $n = 1$ corresponds to an exponential profile and $n = 4$ to the familiar de Vaucouleurs profile (de Vaucouleurs 1948). The factor b_n, is chosen such that the effective radius r_e encloses half of the total luminosity. For the expected range of Sérsic indices, this factor can be approximated by the relation $b_n = 0.868n - 0.142$ (Caon et al. 1993). We convert the projected surface mass densities discussed in Section 3 to a V-band surface brightness profile assuming a stellar age of 10^{10} yr and solar metallicity $Z_\odot = 0.02$ (Bruzual & Charlot 2003) which is then fitted with a Sérsic function [see Naab & Trujillo (2006) for details of the fitting procedure]. Those population properties are reasonable for present day massive ellipticals (Thomas et al. 2010) but not necessarily so for higher redshifts. However, details of the choice of population age and abundance are unimportant for the determination of the profile shape (which are the same as for the surface density profiles) as long as

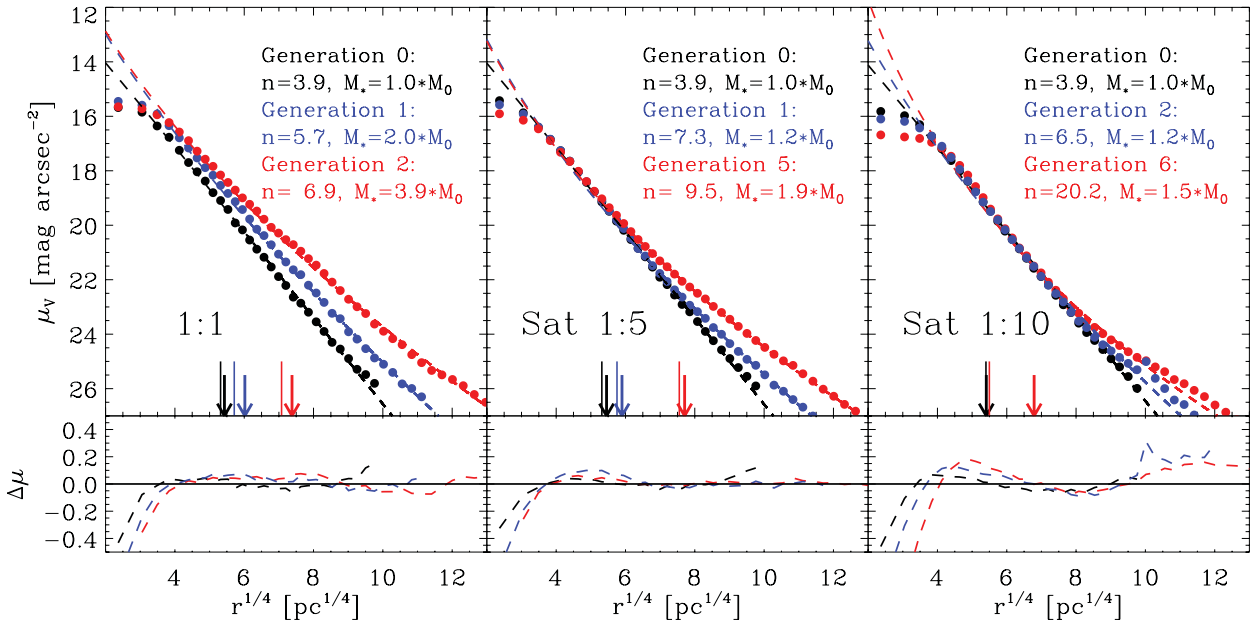

Figure 4. Surface brightness profiles $\mu_V(r)$ of the fiducial two-component 1:1 (left), 1:5 (middle) and 1:10 (right) merger remnants as a function of radius for the initial conditions (black circles), the first merger generation (blue circles, for 1:10 we show the second generation) and the final remnants (red circles). The overplotted dashed lines show the best-fitting Sérsic function for the outer profiles. The data were fitted from $0.02r_e$ to either $10r_e$ or a limiting surface brightness of $m_V = 27\,\mathrm{mag\,arcsec^{-2}}$. The residuals $\Delta\mu < 0.2\,\mathrm{mag\,arcsec^{-2}}$ (lower panels) are small, except for the 1:10 case, which cannot be reasonably well fitted anymore for late generations ($n > 20$) The fitted effective radii $r_{e,\,\mathrm{fit}}$ (short vertical lines) are slightly smaller than the projected half-mass radii r_e (arrows). For minor mergers – 1:5 and 1:10 – the best–fitting Sérsic index n increases rapidly as the mass added in minor mergers grows. Note that for minor mergers, the central surface densities decline the most even as the outer surface densities (and Sérsic indices) increase.

assume a constant mass-to-light ratio (for the stellar component) with radius.

Fig. 4 shows examples of the Sérsic fits to the surface brightness profiles and the residuals of our fiducial bulge+halo mergers with mass-ratios of 1:1 (left), 1:5 (middle) and 1:10 (right). The profiles are fitted from $0.02r_e$ to either $10r_e$ or to a limiting surface brightness of $m_V = 27$ mag arcsec^{-2} (Trujillo et al. 2004; Kormendy et al. 2009). The residuals are very small ($\Delta\mu < 0.2$ mag arcsec^{-2}), except for the innermost regions, where the profiles are affected by insufficient sampling, softening and relaxation effects. The initial Hernquist spheres (black circles in all panels) have a Sérsic index of $n = 3.9$ (see also Naab & Trujillo 2006). In all cases the fitted Sérsic profiles overestimate the central surface brightness leading to a slightly smaller fitted effective radius $r_{e,\,\mathrm{fit}}$ (narrow vertical lines at the bottom of each surface brightness panel) than the projected half-mass radius r_e (corresponding arrows) presented in Fig. 2. The differences are small and do not affect any conclusions in the paper.

In the case of 1:1 mergers of two-component models (left-hand panel, Fig 4), we can see that the profile shape hardly changes for the remnants. The Sérsic index increases weakly from $n = 3.9$ to $n = 5.5$ with a corresponding increase of mass by a factor of about 2, hardly enough to explain the very high numbers observers find for large massive elliptical galaxies ($n \sim 10$; see Caon et al. 1993; Kormendy et al. 2009). This picture changes dramatically for minor mergers where the Sérsic index increases rapidly to values of $n \sim 10$ for a similar increase in mass. This is a direct consequence of the different evolution of the surface density profiles discussed in Section 4.

In Fig. 5 we show, for all fiducial bulge-only and bulge+halo models, the evolution of the Sérsic index as a function of the assembled bound stellar mass. There is only a moderate increase in Sérsic index for the equal-mass mergers. In contrast, after two generations of 1:5 mergers with a mass increase of only 40 per cent, the Sérsic index can be $n > 7$ (for the bulge+halo model) and the final remnant reaches values of $n \sim 9.5$, which is in the range of the observed present-day massive elliptical galaxies (Caon et al. 1993; Kormendy et al. 2009). The corresponding bulge-only minor merger scenarios (red and green dashed lines in Fig. 5) show similar but weaker trends yielding final Sérsic indices of $n \sim 7.5$. Still, the overall evolution is much faster for two-component models. This again indicates that the merger mass-ratio and dark matter haloes play an important role as they increase the effect of stripping at large radii in a way that the accreted stellar mass assembles at the 'right' regions of the host galaxy.

6 EVOLUTION OF DARK MATTER FRACTIONS

In this section, we investigate the dark matter fractions within the effective radii of our simulated merger remnants in the light of recent lensing observations, which predict an increasing dark matter fraction for more massive ellipticals (Auger et al. 2010; Barnabè et al. 2011), dynamical modelling (Gerhard et al. 2001; Cappellari et al. 2012a) and the possibly low dark matter fractions in high-redshift galaxies (Toft et al. 2012). The dark matter fractions f_{dm} for all bulge+halo simulations

$$f_{\mathrm{dm}}(r < r_{50}) = M_{\mathrm{dm}}(r < r_{50})/M_{\mathrm{tot}}(r < r_{50}) \qquad (2)$$

are shown in Fig. 6 as a function of assembled stellar mass. Here r_{50} denotes the spherical half-mass radius of the stellar component, and M_{dm} and M_{tot} are the halo mass and total mass within r_{50}. We have already explained how the observable f_{dm} will increase simply by accounting, when the stars are added far out in the dark matter halo. The dark matter fraction increases rapidly with each subsequent

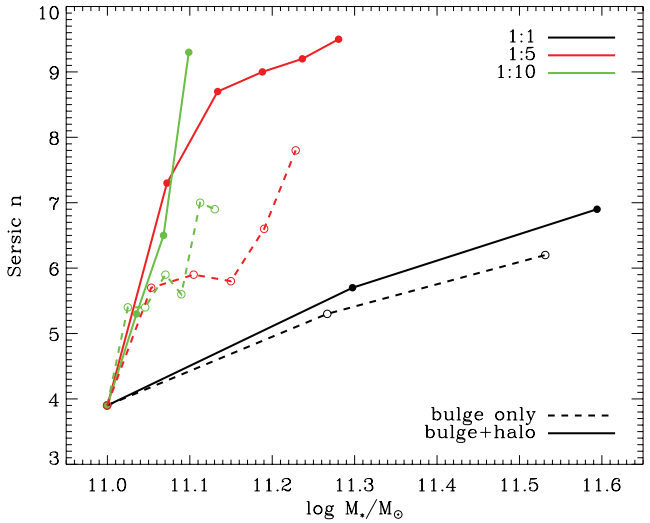

Figure 5. Evolution of the Sérsic indices for all fiducial major and minor merger remnants shown in Fig. 4 as a function of bound stellar mass (the evolution for compact satellites is similar). All equal-mass mergers show a very weak evolution (black lines). Lower mass-ratios lead to a stronger evolution for 1:5 (red dashed) and 1:10 (green dashed) bulge-only models. The presence of dark matter haloes even enhances this effect as more stars are deposited at large radii (red and green solid lines). The 1:5 two-component model shows the strongest evolution reaching values of $n > 9$ after a mass increase of only 50 per cent. For 1:10 mergers we only show the first generations with reasonable Sérsic fits. Later generations cannot be accurately fitted anymore (see Fig. 4).

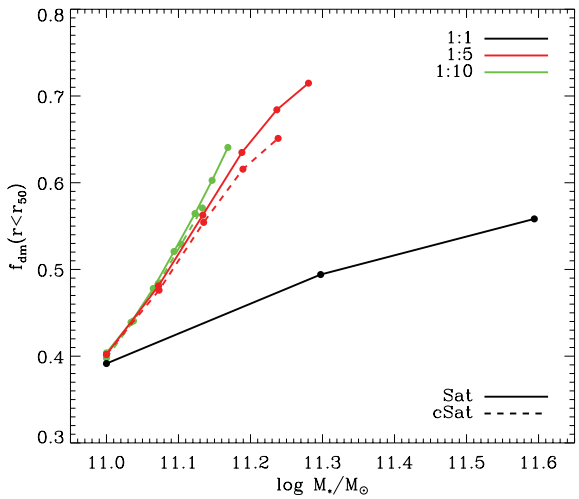

Figure 6. Evolution of the dark matter fraction, $f_{\rm dm}(r < r_{50}) = M_{\rm dm}(r < r_{50})/M_{\rm tot}(r < r_{50})$, within the spherical half-mass radius r_{50} (which is similar to the half-mass radius) for all bulge+halo models as a function of bound stellar mass of the merger remnants. Equal-mass mergers show a weak increase of $f_{\rm dm}$. A very rapid increase of $f_{\rm dm}$ is found for 1:5 (red) and 1:10 (green) mergers, with a similar evolution for compact satellites (dashed lines). The evolution of $f_{\rm dm}$ for 1:5 mergers with mass is very similar to 1:10 mergers indicating that less events results in similar change of $f_{\rm dm}$.

minor merger generation regardless of the mass-ratio. For a mass increase of a factor of 2, the dark matter fractions increases by almost a factor of 2 from ∼40 to $\gtrsim$70 per cent for minor mergers whereas equal-mass mergers only an increase to ∼55 per cent. The strong evolution with added mass for minor mergers is a consequence of the rapid size growth (Fig. 2), which is in good agreement with (Nipoti et al. 2009b). The evolution of $f_{\rm dm}$ correlates with the radii of the merger remnants. Therefore, the 1:5 scenario with more compact satellites (red dashed line), which shows slightly weaker size growth than the fiducial case (Fig. 2), also has a slightly lower dark matter fraction. On the other hand, the 1:10 bulge+halo remnants grow rapidly in size and therefore have the highest dark matter fractions. It is easy to understand this trend. As noted, the dark matter is not pushed inwards; rather we are adding stars to the outer, dark matter-dominated parts of galaxies, so naturally the amount of dark matter within the stars increases. A detailed analysis of this process can be found in Hilz et al. (2012).

7 DISCUSSION AND CONCLUSION

We present idealized binary merger simulations of spheroidal galaxies with initial mass-ratios of 1:1, 1:5 and 1:10 represented by pure bulges and bulges embedded in dark matter haloes. The 1:5 mass-ratio is of particular interest as it is similar to the average mass-weighted galaxy merger mass-ratio driving the assembly of massive galaxies recently published cosmological simulations and therefore those minor mergers (or intermediate mass-ratio mergers, traditionally all mergers with mass ratios smaller than 1:4 are called minor mergers) represent a typical growth mode (Gabor & Davé 2012; Lackner et al. 2012; Oser et al. 2012). With this study we aim at assessing the effect of pure collisionless major and minor mergers on the structural evolution for an already existent, observed, high-redshift population of compact and massive galaxies [see e.g. Bournaud, Jog & Combes (2007) for a discussion on the effect of repeated minor mergers on discs].

Confirming earlier studies, we find that major mergers alone cannot explain the observed size growth but minor mergers with mass-ratios of 1:5 or 1:10 show a significantly stronger size growth per added stellar mass (Khochfar & Silk 2006; Naab et al. 2009; Nipoti et al. 2009a; Hopkins et al. 2010; Hilz et al. 2012; Oser et al. 2012). This effect is slightly enhanced for more diffuse satellites and significantly enhanced if the galaxies are surrounded by dark matter haloes. In these cases, the satellite stars are more efficiently stripped at larger radii, either because they are less bound or because they orbit in the deeper potential wells of the dark matter haloes. The latter effect [see Hilz et al. (2012) for a detailed discussion] leads to an inside-out size growth of $r \propto M^{2.3}$ already for mergers with a mass-ratio of 1:5, in agreement with observations (van Dokkum et al. 2010; Szomoru et al. 2012). Overall, the picture is very similar to the dynamical friction-driven galactic cannibalism described by Hausman & Ostriker (1978) as an explanation for BCG properties (Ruszkowski & Springel 2009; Laporte et al. 2012).

The inside-out assembly of mass at larger radii results in a significant change of the surface density profiles which is here quantified by an increase of the Sérsic index n. Starting at a fiducial value of $n = 4$, the increase is weak for major mergers but very strong for minor mergers of galaxies embedded in dark matter haloes. In the most extreme case, only two 1:5 mergers of bulges with dark matter haloes change the Sérsic index from $n \sim 4$ to $n \sim 8.5$ at a concurrent stellar mass increase of only 40 per cent. We note that $n = 4$ is the fiducial starting point of the specific simulation setup we have chosen. Qualitatively a similar increase in Sérsic index is expected for smaller, and probably more realistic, starting values of $n \sim 2$ for quiescent high-redshift galaxies. In this case, the maximum Sérsic index might not reach as high values as presented here but more accurate predictions are beyond the scope of idealized collisionless studies like the one presented here. Major merger

scenarios with disc-like progenitors do also result in an increase of the Sérsic index but accompanied by a very weak size increase or even a reduction in size in the presence of gas (Cox et al. 2006; Naab & Trujillo 2006; Robertson et al. 2006; Hopkins et al. 2008; Wuyts et al. 2010). Here the increase in Sérsic index is partly driven by dissipative processes at the centre of the remnants. Consistent with the results presented here, even considering subsequent 'dry' major mergers keep the Sérsic indices for the main stellar body low at $n \lesssim 5$ (Naab & Trujillo 2006; Hopkins et al. 2009b). Therefore, a minor merger-driven scenario – the late addition of old stars at large radii – provides a powerful explanation for the predominance of high Sérsic indices of present-day large and massive ellipticals (Graham, Trujillo & Caon 2001; Trujillo et al. 2004; Kormendy et al. 2009; Hoyos et al. 2011; Kormendy & Bender 2012), some of which are most likely the descendants of compact 'red and dead' flattened high-redshift galaxies with lower Sérsic indices (van Dokkum et al. 2008; van der Wel et al. 2009b, 2011; Bundy et al. 2010; Wuyts et al. 2010; Buitrago et al. 2013; Wuyts et al. 2011; Szomoru et al. 2012).

Naturally, major mergers are also expected to happen during the assembly of massive galaxies. There is direct and indirect observational evidence for this but the expected rates are low ($\sim$0.5–2 since $z \sim 2$) (Bell et al. 2006a; McIntosh et al. 2008; van der Wel et al. 2009b; Robaina et al. 2010; Williams et al. 2011; López-Sanjuan et al. 2012; Man et al. 2012; Newman et al. 2012). A major merger will definitely dominate the late mass assembly history of the galaxy with a significant impact on its abundance gradients, kinematics and, eventually, morphology (White 1978; Naab, Khochfar & Burkert 2006; Bois et al. 2011). However, as we have shown here, the expected evolution in size, surface density profile shapes and, eventually, dark matter fraction will be only moderate and not sufficient to evolve the compact high-redshift population into present-day ellipticals. Another argument against major mergers driving the size evolution is the apparent absence (or very low number) of massive compact galaxies in the present-day Universe (Trujillo et al. 2009; Taylor et al. 2010). Due to the low rates, a significant number of massive galaxies will not have experienced any major merger since $z \sim 2$ and would remain compact (Bezanson et al. 2009). Nevertheless, a few massive compact have been found which eventually are relics of the high-redshift population or have formed recently in a similar manner (Valentinuzzi et al. 2010; Ferré-Mateu et al. 2012; Jiang et al. 2012; Trujillo et al. 2012). Consistent with our framework these galaxies have low Sérsic indices and our model predicts lower dark matter fractions compared to normal-sized present-day giant elliptical galaxies of similar mass.

The evolution of dark matter fractions within the observable stellar half-mass radius is also significantly different for major and minor mergers. In the equal-mass mergers presented here the dark matter fraction increases from the fiducial starting value of $\sim$40 to $\sim$48 per cent for a stellar mass increase of a factor of 2. This increase is driven by mixing processes during the violent merger process which lead to a real change in the radial distribution of luminous and dark matter (Hilz et al. 2012, see also Boylan-Kolchin et al. 2005). For the same increase in mass, minor mergers (e.g. 1:5) result in a four times stronger increase of the dark matter fraction (from $\sim$40 to $\gtrsim$70 per cent). Here the host galaxy structure is only weakly affected but the effective radius of the stellar distribution increases significantly into regions which were ab initio dominated by dark matter. Therefore, only the ruler with which the galaxies are measured is changing (Cenarro & Trujillo 2009; Hopkins et al. 2009b; Lackner & Ostriker 2010; Hilz et al. 2012). We note that the exact numbers for the final dark matter fractions are determined by our choice of the initial dark matter fraction. Our fiducial starting value of $\sim$40 per cent might in reality be lower for massive high-redshift galaxies but also in this case we expect similar trends. There is evidence for the presence of dark matter in present-day massive ellipticals; however, the exact amount is uncertain (Gerhard et al. 2001; Thomas et al. 2009, 2011; Cappellari et al. 2012a). Most recent lensing observations indicate dark matter fractions (with large uncertainties) in the range of 20–50 per cent with higher fractions for more massive galaxies (Auger et al. 2010; Barnabè et al. 2011). These trends are easy to reconcile in the context of an evolutionary scenario where the early formation of ellipticals is dominated by a dissipative formation with little dark matter at the centre [see (Toft et al. 2012) for tentative observational evidence] followed by a dissipationless assembly dominated by minor mergers naturally increasing the dark matter fractions. This increase would be larger for more massive galaxies which assemble more mass by late stellar mergers (see e.g. De Lucia et al. 2006; De Lucia & Blaizot 2007; Guo & White 2008; Oser et al. 2010, 2012; Lackner et al. 2012). However, predicted dark matter fractions depend sensitively on assumptions about the stellar initial mass function and recent evidence for rising stellar mass-to-light ratios with stellar mass leave less room for the presence of dark matter (van Dokkum & Conroy 2010, 2012; Cappellari et al. 2012b; Conroy & van Dokkum 2012; Ferreras et al. 2012).

More quantitative predictions, some based on simple binary merger simulations of spheroids similar to the ones presented here, in a cosmological context have been attempted and come to varying conclusions; some agree with observations (Ciotti et al. 2007), some highlight possible tension with observational trends (Nipoti et al. 2009a,b; Cimatti et al. 2012; Nipoti et al. 2012; Quilis & Trujillo 2012). However, the quantitative predictive power of such studies is limited by construction as a realistic cosmological assembly of massive galaxies is very complex and many details depend on the model assumptions about the structure of the galaxies and the satellites, galaxy orbits, gas fractions, merger rates, etc. Qualitatively, however, our results are in good agreement with high-resolution cosmological simulations (Feldmann et al. 2010; Lackner et al. 2012; Oser et al. 2012), which are supposedly the method of choice to evaluate these processes in more detail in the future.

The predictions of this simple – dark matter assisted – minor merger-driven evolution model are in good qualitative agreement with careful observations of the structural redshift evolution of early-type galaxies (van Dokkum et al. 2010; Buitrago et al. 2013; Weinzirl et al. 2011; McLure et al. 2012; Szomoru et al. 2012). We note here that we have tested for the extreme case of compact progenitors. A significant fraction of high-redshift ellipticals have larger sizes (Mancini et al. 2010; Szomoru et al. 2012) and would require relatively little evolution and less mergers. All the above effects are expected to be stronger for more massive galaxies which are expected to have a larger fraction of their stars acquired in accretion events. The most extreme cases would be central in galaxy clusters (Ostriker & Hausman 1977; Dubinski 1998; De Lucia & Blaizot 2007; Ruszkowski & Springel 2009; Laporte et al. 2012).

If we are right, then certain definite and testable predictions can be made about the properties of the outer parts ($r > r_e$) of normal giant ellipticals: Since they are the result of the accretion of low-mass systems they should have considerably lower metallicities than the inner parts. Steeper gradients at large radii then might imply a formation history dominated by minor mergers (White 1978; Kobayashi 2004, see however Pipino et al. 2010 for an alternative view). The stellar orbits at large radii should become radially biased

(Hilz et al. 2012) and the dark matter fractions of massive ellipticals should increase rapidly at large radii.

ACKNOWLEDGMENTS

We thank the anonymous referee for valuable comments on the manuscript. We also thank Simon White for valuable discussions. This research was supported by the DFG cluster of excellence 'Origin and Structure of the Universe' and the DFG priority programme SPP 1177.

REFERENCES

Auger M. W., Treu T., Bolton A. S., Gavazzi R., Koopmans L. V. E., Marshall P. J., Moustakas L. A., Burles S., 2010, ApJ, 724, 511
Auger M. W., Treu T., Brewer B. J., Marshall P. J., 2011, MNRAS, 411, L6
Barnabè M., Czoske O., Koopmans L. V. E., Treu T., Bolton A. S., 2011, MNRAS, 415, 2215
Bell E. F. et al., 2006a, ApJ, 640, 241
Bell E. F., Phleps S., Somerville R. S., Wolf C., Borch A., Meisenheimer K., 2006b, ApJ, 652, 270
Bezanson R., van Dokkum P. G., Tal T., Marchesini D., Kriek M., Franx M., Coppi P., 2009, ApJ, 697, 1290
Bois M. et al., 2011, MNRAS, 416, 1654
Bournaud F., Jog C. J., Combes F., 2007, A&A, 476, 1179
Bournaud F. et al., 2011, ApJ, 730, 4
Boylan-Kolchin M., Ma C., Quataert E., 2005, MNRAS, 362, 184
Brinchmann J., Ellis R. S., 2000, ApJ, 536, L77
Bruzual G., Charlot S., 2003, MNRAS, 344, 1000
Buitrago F., Trujillo I., Conselice C. J., Bouwens R. J., Dickinson M., Yan H., 2008, ApJ, 687, L61
Buitrago F., Trujillo I., Conselice C. J., Haeussler B., 2013, MNRAS, 428, 1460
Bundy K. et al., 2010, ApJ, 719, 1969
Burkert A., Naab T., Johansson P. H., Jesseit R., 2008, ApJ, 685, 897
Caon N., Capaccioli M., D'Onofrio M., 1993, MNRAS, 265, 1013
Cappellari M. et al., 2012a, arXiv:1208.3522
Cappellari M. et al., 2012b, Nat, 484, 485
Carrasco E. R., Conselice C. J., Trujillo I., 2010, MNRAS, 405, 2253
Cenarro A. J., Trujillo I., 2009, ApJ, 696, L43
Cimatti A. et al., 2008, A&A, 482, 21
Cimatti A., Nipoti C., Cassata P., 2012, MNRAS, 422, L62
Ciotti L., Lanzoni B., Volonteri M., 2007, ApJ, 658, 65
Cole S., Lacey C. G., Baugh C. M., Frenk C. S., 2000, MNRAS, 319, 168
Conroy C., van Dokkum P., 2012, ApJ, 760, 71
Covington M. D., Primack J. R., Porter L. A., Croton D. J., Somerville R. S., Dekel A., 2011, MNRAS, 415, 3135
Cox T. J., Dutta S. N., Di Matteo T., Hernquist L., Hopkins P. F., Robertson B., Springel V., 2006, ApJ, 650, 791
Crocker A. et al., 2012, MNRAS, 421, 1298
Daddi E. et al., 2005, ApJ, 626, 680
Damjanov I. et al., 2009, ApJ, 695, 101
De Lucia G., Blaizot J., 2007, MNRAS, 375, 2
De Lucia G., Springel V., White S. D. M., Croton D., Kauffmann G., 2006, MNRAS, 366, 499
de Vaucouleurs G., 1948, Ann. Astrophys., 11, 247
Dekel A., Cox T. J., 2006, MNRAS, 370, 1445
Dekel A., Sari R., Ceverino D., 2009, ApJ, 703, 785
Domínguez Sánchez H. et al., 2011, MNRAS, 417, 900
Dubinski J., 1998, ApJ, 502, 141
Duc P.-A. et al., 2011, MNRAS, 417, 863
Edwards L. O. V., Patton D. R., 2012, MNRAS, 425, 287
Faber S. M. et al., 2007, ApJ, 665, 265
Farouki R. T., Shapiro S. L., Duncan M. J., 1983, ApJ, 265, 597
Feldmann R., Carollo C. M., Mayer L., Renzini A., Lake G., Quinn T., Stinson G. S., Yepes G., 2010, ApJ, 709, 218
Feldmann R., Carollo C. M., Mayer L., 2011, ApJ, 736, 88
Ferré-Mateu A., Vazdekis A., Trujillo I., Sánchez-Blázquez P., Ricciardelli E., de la Rosa I. G., 2012, MNRAS, 423, 632
Ferreras I., La Barbera F., de Carvalho R. R., de la Rosa I. G., Vazdekis A., Falcon-Barroso J., Ricciardelli E., 2012, arXiv:1206.1594
Franx M., van Dokkum P. G., Schreiber N. M. F., Wuyts S., Labbé I., Toft S., 2008, ApJ, 688, 770
Gabor J. M., Davé R., 2012, MNRAS, 427, 1816
Gerhard O., Kronawitter A., Saglia R. P., Bender R., 2001, AJ, 121, 1936
Governato F., Willman B., Mayer L., Brooks A., Stinson G., Valenzuela O., Wadsley J., Quinn T., 2007, MNRAS, 374, 1479
Graham A. W., Trujillo I., Caon N., 2001, AJ, 122, 1707
Guo Q., White S. D. M., 2008, MNRAS, 384, 2
Guo Q. et al., 2011, MNRAS, 413, 101
Guo Y. et al., 2009, MNRAS, 398, 1129
Hausman M. A., Ostriker J. P., 1978, ApJ, 224, 320
Hernquist L., 1990, ApJ, 356, 359
Hilz M., Naab T., Ostriker J. P., Thomas J., Burkert A., Jesseit R., 2012, MNRAS, 425, 3119
Hopkins P. F., Cox T. J., Hernquist L., 2008, ApJ, 689, 17
Hopkins P. F., Bundy K., Murray N., Quataert E., Lauer T. R., Ma C.-P., 2009a, MNRAS, 398, 898
Hopkins P. F., Hernquist L., Cox T. J., Keres D., Wuyts S., 2009b, ApJ, 691, 1424
Hopkins P. F., Bundy K., Hernquist L., Wuyts S., Cox T. J., 2010, MNRAS, 401, 1099
Hoyos C. et al., 2011, MNRAS, 411, 2439
Hyde J. B., Bernardi M., 2009, MNRAS, 394, 1978
Jiang F., van Dokkum P., Bezanson R., Franx M., 2012, ApJ, 749, L10
Joung M. R., Cen R., Bryan G. L., 2009, ApJ, 692, L1
Kauffmann G., 1996, MNRAS, 281, 487
Kauffmann G. et al., 2012, MNRAS, 422, 997
Kereš D., Katz N., Weinberg D. H., Davé R., 2005, MNRAS, 363, 2
Kereš D., Katz N., Fardal M., Davé R., Weinberg D. H., 2009, MNRAS, 395, 160
Khochfar S., Silk J., 2006, ApJ, 648, L21
Kobayashi C., 2004, MNRAS, 347, 740
Kormendy J., Bender R., 2012, ApJS, 198, 2
Kormendy J., Fisher D. B., Cornell M. E., Bender R., 2009, ApJS, 182, 216
Kriek M. et al., 2006, ApJ, 649, L71
Kriek M., van der Wel A., van Dokkum P. G., Franx M., Illingworth G. D., 2008, ApJ, 682, 896
Kriek M., van Dokkum P. G., Labbé I., Franx M., Illingworth G. D., Marchesini D., Quadri R. F., 2009, ApJ, 700, 221
Lackner C. N., Ostriker J. P., 2010, ApJ, 712, 88
Lackner C. N., Cen R., Ostriker J. P., Joung M. R., 2012, MNRAS, 425, 641
Laporte C. F. P., White S. D. M., Naab T., Ruszkowski M., Springel V., 2012, MNRAS, 424, 747
Longhetti M. et al., 2007, MNRAS, 374, 614
López-Sanjuan C., Balcells M., Pérez-González P. G., Barro G., García-Dabó C. E., Gallego J., Zamorano J., 2010, ApJ, 710, 1170
López-Sanjuan C. et al., 2012, A&A, 548, A7
Lotz J. M., Jonsson P., Cox T. J., Croton D., Primack J. R., Somerville R. S., Stewart K., 2011, ApJ, 742, 103
Malin D. F., Carter D., 1983, ApJ, 274, 534
Man A. W. S., Toft S., Zirm A. W., Wuyts S., van der Wel A., 2012, ApJ, 744, 85
Mancini C. et al., 2010, MNRAS, 401, 933
Mármol-Queraltó E., Trujillo I., Pérez-González P. G., Varela J., Barro G., 2012, MNRAS, 422, 2187
Matteucci F., Francois P., 1989, MNRAS, 239, 885
McIntosh D. H., Guo Y., Hertzberg J., Katz N., Mo H. J., van den Bosch F. C., Yang X., 2008, MNRAS, 388, 1537
McLure R. J. et al., 2012, MNRAS, 428, 1088
Miller R. H., Smith B. F., 1980, ApJ, 235, 421
Misgeld I., Hilker M., 2011, MNRAS, 414, 3699
Mo H. J., Mao S., White S. D. M., 1998, MNRAS, 295, 319
Moster B. P., Naab T., White S. D. M., 2012, arXiv:1205.5807

Naab T., Burkert A., 2003, ApJ, 597, 893
Naab T., Ostriker J. P., 2006, MNRAS, 366, 899
Naab T., Ostriker J. P., 2009, ApJ, 690, 1452
Naab T., Trujillo I., 2006, MNRAS, 369, 625
Naab T., Khochfar S., Burkert A., 2006, ApJ, 636, L81
Naab T., Johansson P. H., Ostriker J. P., Efstathiou G., 2007, ApJ, 658, 710
Naab T., Johansson P. H., Ostriker J. P., 2009, ApJ, 699, L178
Nelson A. F., Wetzstein M., Naab T., 2009, ApJS, 184, 326
Newman A. B., Ellis R. S., Bundy K., Treu T., 2012, ApJ, 746, 162
Nipoti C., Londrillo P., Ciotti L., 2003, MNRAS, 342, 501
Nipoti C., Treu T., Auger M. W., Bolton A. S., 2009a, ApJ, 706, L86
Nipoti C., Treu T., Bolton A. S., 2009b, ApJ, 703, 1531
Nipoti C., Treu T., Leauthaud A., Bundy K., Newman A. B., Auger M. W., 2012, MNRAS, 422, 1714
Onodera M. et al., 2012, ApJ, 755, 26
Oser L., Ostriker J. P., Naab T., Johansson P. H., Burkert A., 2010, ApJ, 725, 2312
Oser L., Naab T., Ostriker J. P., Johansson P. H., 2012, ApJ, 744, 63
Ostriker J. P., 1980, Comments Astrophys., 8, 177
Ostriker J. P., Hausman M. A., 1977, ApJ, 217, L125
Pipino A., D'Ercole A., Chiappini C., Matteucci F., 2010, MNRAS, 407, 1347
Prantzos N., Aubert O., 1995, A&A, 302, 69
Quilis V., Trujillo I., 2012, ApJ, 752, L19
Ricciardelli E., Trujillo I., Buitrago F., Conselice C. J., 2010, MNRAS, 406, 230
Robaina A. R., Bell E. F., van der Wel A., Somerville R. S., Skelton R. E., McIntosh D. H., Meisenheimer K., Wolf C., 2010, ApJ, 719, 844
Robertson B., Cox T. J., Hernquist L., Franx M., Hopkins P. F., Martini P., Springel V., 2006, ApJ, 641, 21
Ruszkowski M., Springel V., 2009, ApJ, 696, 1094
Saglia R. P. et al., 2010, A&A, 524, A6
Saracco P., Longhetti M., Andreon S., 2009, MNRAS, 392, 718
Saracco P., Gargiulo A., Longhetti M., 2012, MNRAS, 422, 3107
Schweizer F., Seitzer P., 1992, AJ, 104, 1039
Searle L., Sargent W. L. W., Bagnuolo W. G., 1973, ApJ, 179, 427
Sersic J. L., 1968, Atlas de galaxias australes
Shen S., Mo H. J., White S. D. M., Blanton M. R., Kauffmann G., Voges W., Brinkmann J., Csabai I., 2003, MNRAS, 343, 978
Springel V., 2005, MNRAS, 364, 1105
Szomoru D., Franx M., van Dokkum P. G., 2012, ApJ, 749, 121
Tal T., Wake D. A., van Dokkum P. G., van den Bosch F. C., Schneider D. P., Brinkmann J., Weaver B. A., 2012, ApJ, 746, 138
Taylor E. N., Franx M., Glazebrook K., Brinchmann J., van der Wel A., van Dokkum P. G., 2010, ApJ, 720, 723
Thomas J., Saglia R. P., Bender R., Thomas D., Gebhardt K., Magorrian J., Corsini E. M., Wegner G., 2009, ApJ, 691, 770
Thomas D., Maraston C., Schawinski K., Sarzi M., Silk J., 2010, MNRAS, 404, 1775
Thomas J. et al., 2011, MNRAS, 415, 545
Tiret O., Salucci P., Bernardi M., Maraston C., Pforr J., 2011, MNRAS, 411, 1435
Toft S., van Dokkum P., Franx M., Thompson R. I., Illingworth G. D., Bouwens R. J., Kriek M., 2005, ApJ, 624, L9
Toft S. et al., 2007, ApJ, 671, 285
Toft S., Gallazzi A., Zirm A., Wold M., Zibetti S., Grillo C., Man A., 2012, ApJ, 754, 3
Tran K.-V. H., van Dokkum P., Franx M., Illingworth G. D., Kelson D. D., Schreiber N. M. F., 2005, ApJ, 627, L25
Treu T., Ellis R. S., Liao T. X., van Dokkum P. G., 2005, ApJ, 622, L5
Trujillo I., Erwin P., Asensio Ramos A., Graham A. W., 2004, AJ, 127, 1917
Trujillo I. et al., 2006, ApJ, 650, 18
Trujillo I., Conselice C. J., Bundy K., Cooper M. C., Eisenhardt P., Ellis R. S., 2007, MNRAS, 382, 109
Trujillo I., Cenarro A. J., de Lorenzo-Cáceres A., Vazdekis A., de la Rosa I. G., Cava A., 2009, ApJ, 692, L118
Trujillo I., Ferreras I., de La Rosa I. G., 2011, MNRAS, 415, 3903
Trujillo I., Carrasco E. R., Ferré-Mateu A., 2012, ApJ, 751, 45
Valentinuzzi T. et al., 2010, ApJ, 721, L19
van der Wel A., Holden B. P., Zirm A. W., Franx M., Rettura A., Illingworth G. D., Ford H. C., 2008, ApJ, 688, 48
van der Wel A., Bell E. F., van den Bosch F. C., Gallazzi A., Rix H., 2009a, ApJ, 698, 1232
van der Wel A., Rix H.-W., Holden B. P., Bell E. F., Robaina A. R., 2009b, ApJ, 706, L120
van der Wel A. et al., 2011, ApJ, 730, 38
van Dokkum P. G., 2005, AJ, 130, 2647
van Dokkum P. G., Conroy C., 2010, Nat, 468, 940
van Dokkum P., Conroy C., 2012, ApJ, 760, 70
van Dokkum P. G. et al., 2008, ApJ, 677, L5
van Dokkum P. G. et al., 2010, ApJ, 709, 1018
Villumsen J. V., 1983, MNRAS, 204, 219
Wang J. et al., 2011, MNRAS, 412, 1081
Weinzirl T. et al., 2011, ApJ, 743, 87
Wetzstein M., Nelson A. F., Naab T., Burkert A., 2009, ApJS, 184, 298
Whitaker K. E., van Dokkum P. G., 2008, ApJ, 676, L105
Whitaker K. E., Kriek M., van Dokkum P. G., Bezanson R., Brammer G., Franx M., Labbé I., 2012, ApJ, 745, 179
White S. D. M., 1978, MNRAS, 184, 185
White S. D. M., 1979, MNRAS, 189, 831
Williams R. J., Quadri R. F., Franx M., van Dokkum P., Toft S., Kriek M., Labbé I., 2010, ApJ, 713, 738
Williams R. J., Quadri R. F., Franx M., 2011, ApJ, 738, L25
Wuyts S., Cox T. J., Hayward C. C., Franx M., Hernquist L., Hopkins P. F., Jonsson P., van Dokkum P. G., 2010, ApJ, 722, 1666
Wuyts S. et al., 2011, ApJ, 742, 96
Yang X., Mo H. J., van den Bosch F. C., Zhang Y., Han J., 2012, ApJ, 752, 41
Young L. M. et al., 2011, MNRAS, 414, 940
Zirm A. W. et al., 2007, ApJ, 656, 66

This paper has been typeset from a TEX/LATEX file prepared by the author.